https://doi.org/10.5194/egusphere-2026-4533
Preprint. Discussion started: 26 August 2026

In situ observations of gravity waves over tropical cyclone Hinnamnor (2022) suggest that TC gravity wave amplitudes are underestimated in ERA5 reanalysis

Carly KleinStern[1], Benjamin Clouser[2], Thaopaul Bui[3, 4], Jonathan Dean-Day[3, 4], Adrien Desmoulin[2], James Franke[2], Hisashi Nakamura[5], Rei Ueyama[3], Shingo Watanabe[6,7], and Elisabeth Moyer[2]

[1]University of Chicago, Dept. of Physics, Chicago, IL, USA 60637
[2]University of Chicago, Dept. of the Geophysical Sciences, Chicago, IL, USA 60637
[3]NASA Ames Research Center, Moffett Field, CA, USA 94035
[4]Bay Area Environmental Research Institute, Moffett Field, CA, USA 94035
[5]Research Center for Advanced Science and Technology, The University of Tokyo, Tokyo, Japan
[6]Japan Agency for Marine-Earth Science and Technology (JAMSTEC), Yokohama, Kanagawa, Japan
[7]Advanced Institute for Marine Ecosystem Change (WPI-AIMEC), Tohoku University, Sendai, Miyagi, Japan

Correspondence: C. KleinStern, cckleinstern@uchicago.edu; E. Moyer, moyer@uchicago.edu

Abstract.

Tropical cyclones (TCs) are known to regularly excite near-concentric outwardly radiating gravity waves in the lower stratosphere, with horizontal wavelengths of a few hundred kilometers. These disturbances can potentially drive in situ cirrus production, but their amplitudes have been poorly known: satellite observations produce substantially lower amplitudes than those in models or reanalysis, and there have been few aircraft overflights to provide in situ measurements. We present here data from a new TC overflight of supertyphoon Hinnamnor by the NASA WB-57 in 2022 during ACCLIP (the Asian Summer Monsoon Chemical and CLimate Impact Project). Hinnamnor produced a clear and large gravity wave temperature signal in the lower stratosphere, at 9.6 K peak-to-peak, nearly an order of magnitude larger than typical satellite studies and three times as large as in contemporaneous ERA5 reanalysis. The measured value would fall in the 97th percentile in ERA5, based on a sample of 114 summertime TCs in the Western Pacific basin, which produce near-ubiquitous but weaker concentric gravity waves. A metanalysis and comparison of ERA5 to observed winds suggests that both satellite retrievals and reanalysis underestimate TC gravity wave amplitudes because of resolution constraints. Satellite retrievals dampen short-vertical wavelength

https://doi.org/10.5194/egusphere-2026-4533
Preprint. Discussion started: 26 August 2026

perturbations, while reanalyses fail to capture the rapid intensification of tropical cyclones that is associated with strong gravity wave production. These results imply that high-resolution measurements are needed to quantify the influence of TC-induced gravity waves on the stratospheric water budget.

1 Introduction

Between 80–100 tropical cyclones (TCs) form each year across ocean basins, bringing with them extreme winds and precipitation (Knutson et al., 2010). TCs, defined as rapidly rotating low-pressure systems that derive energy from the ocean surface, play a substantial role in heat transport, a role that may increase as TC intensity is predicted to increase in warmer climate conditions (Emanuel, 2005; Elsner et al., 2008). TCs also regularly produce short-wavelength gravity waves (GWs) at their tops, in concentric rings (Liu et al., 2014; Tratt et al., 2018; Li et al., 2022a) or spiral patterns (Chow et al., 2002; Wu et al., 2022); we use the term "concentric gravity waves" for both cases. Although the contribution of TC-generated gravity waves to driving stratospheric circulation is likely small relative to other sources (Kuester et al., 2008; Jewtoukoff et al., 2013; Wright, 2019), they can affect the structure of the upper troposphere and lower stratosphere (UTLS) and can remove water via in situ cirrus cloud formation (Pandit et al., 2024). Cirrus formation in the temperature minima of gravity waves is a common UTLS phenomenon and is important to both radiation and water budgets (Jensen et al., 2016; Podglajen et al., 2016; Kim et al., 2016; Chang and L'Ecuyer, 2020). The characteristics of TC gravity waves remain poorly known, however, and those characteristics drive both the occurrence of cirrus and the size distribution and other microphysical properties of ice particles (Dinh et al., 2016; Atlas and Bretherton, 2023).

Tropical cyclones produce concentric gravity waves intermittently throughout their lifetime (Wright, 2019; Cullens et al., 2023; Wang et al., 2024). Several satellite-based studies suggest that strong gravity waves are more likely when storms are intensifying, with enhanced gravity wave activity actually preceding the increase in cyclonic wind speeds (e.g. Kim and Chun, 2010; Chane Ming et al., 2014). Hoffmann et al. (2018) suggests that gravity wave production is driven by deep convective towers that are more frequent during intensification. Enhanced gravity wave production during intensification may in turn explain the observed slight dependence of amplitude on TC intensity (e.g. Wang et al., 2024). Analysis of concentric gravity wave features is complicated, however, by the fact that their amplitudes are generally not symmetric in space (e.g. Kim et al., 2009; Gong et al., 2015). Radar and radiosonde case studies suggest amplitudes are stronger at the leading edge of a storm (Sato, 1993) by as much as a factor of two

https://doi.org/10.5194/egusphere-2026-4533
Preprint. Discussion started: 26 August 2026

(Dhaka et al., 2003), but structures are dependent on background wind conditions and on TC location (Wang et al., 2024).

While TC-generated concentric gravity waves have been studied in satellite observations, in reanalyses, and in models, the results vary widely (Table 1). Most published results are case studies of individual TCs, which can differ since convectively generated GWs, unlike topographic GWs, span a large range of phase speeds, frequencies, and horizontal and vertical wavelengths (Fritts and Alexander, 2003). Some general patterns are, however, clear: gravity wave amplitudes are smallest in studies based on satellite observations, and become larger as resolution increases, in particular vertical resolution. Resolution both directly restricts the observable spectrum of gravity waves and, in models, indirectly affects gravity waves by altering fundamental TC physics (Kim et al., 2009).

Satellite-based studies of TC gravity waves typically use NASA's Atmospheric Infrared Sounder (AIRS), which is sensitive to horizontal wavelengths greater than 30–80 km (in the best case, when Level 1B data is used) and vertical wavelengths greater than 12–15 km (Beres et al., 2002; Hoffmann and Alexander, 2009). Weighting functions are retrieval dependent, but in all cases features at smaller scales are attenuated or omitted. AIRS studies typically focus on 30–40 km altitude where signal is strongest, but show amplitudes of only ~1 K. GW amplitudes would be even smaller in the UTLS, the region of concern for cirrus formation. Model studies that coarsen their output using the AIRS weighting function produce amplitudes similar to those observed from AIRS, or even slightly smaller (e.g. Kim et al., 2009; Wu et al., 2015 for TC GWs, or Schroeder et al., 2009; Gong et al., 2015 for non-TC-specific GWs).

Studies based on reanalysis output produce TC gravity wave amplitudes roughly three times larger than in AIRS. Reanalysis models have horizontal resolutions similar to AIRS (~30 km) but finer vertical resolution (0.5–1 km in the lower stratosphere). However, numerical diffusion means that even reanalyses still do not fully resolve gravity waves with vertical wavelengths less than 10 km (Preusse et al., 2014; Pahlavan et al., 2023). Furthermore, while reanalyses produce the TCs seen in observations, with reasonable surface pressures (Kim et al., 2009; Hodges et al., 2017), they do not accurately capture TC physics, producing wind speeds that are too low and too constant (Moon et al., 2020; Roberts et al., 2020; Xu et al., 2024). Baker et al. (2024) argue that a model resolution below ~5 km would be needed to realistically capture observed patterns of rapid TC intensification.

Case studies that simulate individual TCs at finer scales (3–9 km horizontal resolution) tend to produce concentric gravity waves with slightly larger amplitudes than in coarser reanalysis. Those studies that report temperature perturbations directly are shown in Table 1; their mean values are ~25 % larger than in reanalysis. Two of these

https://doi.org/10.5194/egusphere-2026-4533
Preprint. Discussion started: 26 August 2026

Table 1. Characteristics of TC-generated concentric gravity waves in the stratosphere, for studies with reported temperature amplitudes. Where possible, we list amplitude, horizontal and vertical wavelengths (λ_h, λ_v), and period (T). AIRS resolution and detection limits are compiled from Alexander and Barnet (2007) and Hoffmann and Alexander (2009). For nested model studies, we show results from the highest-resolution inner domain. Note that radiosonde GWs are not guaranteed to be concentric. We show results near 35 km altitude other than for studies that report values only in the UTLS (16–18 km), where gravity wave amplitudes are ~50–65 % lower (Kim et al., 2009; Cullens et al., 2023). In most cases amplitudes are estimated from figures by eye. Where systems are anisotropic we choose the maximum peak-to-peak amplitude. Studies are broadly consistent for horizontal wavelengths and periods, but higher-resolution studies show larger gravity wave amplitudes. (The discrepancy would be even stronger were all values reported at the same altitude.)

Study	Method	TC	Alt. (km)	Pk-to-pk amp. (K)	λ_h (km)	λ_v (km)	T (h)
Satellite: horizontal. res. 13–40 km (retrieval dependent), vertical res. 3–15 km *Mean amplitude = 1.2 K*							
Huang et al. (2024)	AIRS	Molave (2020)	30–40	0.8	–	–	–
Cullens et al. (2023)	AIRS	5 TCs in 2018	30–40	0.4	60–300	–	–
Shi et al. (2021)	AIRS	Bejisa (2014)	30-40	1	150–190	16–24	~0.75
Yue et al. (2014)	AIRS	Mahasen (2013)	30–40	1	60–150	–	–
Kim et al. (2009)	AIRS	Ewiniar (2006)	30–40	2–2.5	150–500	–	–
Kuester (2007)	AIRS	Katrina (2005)	30–40	1.5	40–200	~ 0	–
Model (coarsened to AIRS): *Mean amplitude = 1.2 K*							
Wu et al. (2015)	WRF	Mindulle (2004)	33	0.8	100–400	6–12	7–12
Kim et al. (2009)	WRF	Ewiniar (2006)	42	1.5	150–700	–	3–11
Reanalysis: horizontal res. 30 km, vertical res. 0.5–1 km *Mean amplitude = 3.8 K*							
Huang et al. (2024)	ERA5	Molave (2020)	16	2–3	–	–	–
Li et al. (2022a)	ERA5	Chaba (2016)	40	3–4	290	–	–
Kim et al. (2009)	ECMWF	Ewiniar (2006)	42	5.5	200-600	13.5	3–9
High resolution model: horizontal res. 3–9 km, vertical res. 0.5 km *Mean amplitude = 5 K*							
Huang et al. (2024)	WRF	Molave (2020)	15.7	2–4	800–1000	5–8	–
Chane Ming et al. (2019)	WRF	Soudelor (2015)	18–25	5.5	16–700	1.4–5	1–20
Kim et al. (2009)	WRF	Ewiniar (2006)	42	6.5	50–300	10–11	1–2
In situ: horizontal res. 0.2 km (aircraft); vertical res 30 m (radiosonde) *Mean amplitude = 6.5 K*							
Pfister et al. (1993)	Aircraft	Jason (1987)	18.3	4.8	265	0.4	4.5–6
Chane Ming et al. (2002)	Radiosonde	Dina (2002)	17–19	5	500–1900	3.5–4.5	1.3–1.6
This study	Aircraft	Hinnamnor (2022)	18	9.6	560	–	–

https://doi.org/10.5194/egusphere-2026-4533
Preprint. Discussion started: 26 August 2026

are nested model simulations; we show the inner domain. A larger set of case studies report only vertical velocities and periods but are broadly consistent, implying rapid vertical displacements of hundreds of meters and therefore temperature perturbations of a few degrees. High-resolution simulations of TC Humberto (MM5) (Kuester et al., 2008), TC Saomai (Weather Research and Forecasting - WRF) (Kim and Chun, 2010), TC Lekima (WRF) (Wang et al., 2021), and a group of five TCs in 2018 (ECMWF IFS) (Cullens et al., 2023) all find maximum vertical velocities in the UTLS from 0.05–0.6 $\mathrm{ms^{-1}}$ and periods from 0.3–10 h, with higher velocities generally corresponding to shorter periods. These high resolution models appear to have more realistic hurricane physics than do reanalyses. For example, Huang et al. (2024) found that simulations with WRF using a 3 km grid accurately captured the rapid intensification of Hurricane Molave, when wind speeds tripled over three days.

The most definitive estimates of TC gravity wave amplitudes should come from in situ measurements by research aircraft and radiosondes. Aircraft temperature data have effective horizontal resolution of ~5–200 m (from 1–20 Hz data at an airspeed of ~100–200 $\mathrm{ms^{-1}}$); radiosondes have vertical resolution of ~30 m or less (0.17–1 Hz data). However, the regular hurricane monitoring flights by NOAA and other agencies do not reach above the base of the UTLS (Aberson et al., 2006), and radiosonde sampling typically occurs only when a TC passes over an existing station. Aircraft overflights of tropical cyclones are rare. The authors know of only four campaigns with published overflights since the earliest U-2 campaigns of the 1950s–1960s (e.g. Penn, 1964; Koteswaram, 1967), and only one of these produced a reported gravity wave temperature amplitude. In 1987, the ER-2 aircraft overflew cyclone Jason (then a tropical storm on the Saffir-Simpson scale) near Australia during STEP (the Stratosphere-Troposphere Exchange Project) and observed a 4.8 K temperature perturbation interpreted as a TC gravity wave (Pfister et al., 1993, see Fig. S1). Three other campaigns involved TC overflights and reported gravity wave activity but did not quantify UTLS temperature perturbations: APE-THESEO for cyclone Davina in 1999 (Cairo et al., 2008, see Fig. S1), CAMEX-4 for several cyclones in 2001 (Kuester et al., 2008), and HS3 for hurricanes Edouard and Gonzalo in 2012 and 2014 (Braun et al., 2016). Radiosonde observations are also limited. Chane Ming et al. (2002, 2010, 2014) used radiosondes to detect gravity waves above 4 TCs that passed over or near islands with weather stations between 2000–2008, and reported temperature amplitudes of ~5 K and vertical wavelengths of ~1–3 km from TC Tromelin.

One additional aircraft campaign bears mentioning, though it did not focus on tropical cyclones: the 2025 Convective Gravity Waves in the Stratosphere (CG WaveS) mission, based out of Des Moines, Iowa, USA in 2025. This campaign sought to measure gravity waves above continental convective systems using a mid-tropospheric aircraft and lidar for remote temperature measurements. At the time of writing, results have not yet been published.

https://doi.org/10.5194/egusphere-2026-4533
Preprint. Discussion started: 26 August 2026

This study reports on in situ measurements during a new TC overflight, of cyclone Hinnamnor by the NASA WB-57 aircraft during the Asian Summer Monsoon Chemical and CLimate Impact Project (ACCLIP, summer 2022). These measurements represent an important addition to our limited in situ sampling of TC-generated gravity waves in the UTLS. In the remainder of this paper, Sect. 2 introduces the ACCLIP campaign and the in situ and reanalysis datasets used in this study; Sect. 3.1 describes the Hinnamnor overflight and its signature of gravity wave activity; Sect. 3.2 and 3.3 compare the aircraft data to the representation of Hinnamnor in ERA5 (the European Center for Medium-range Weather Forecasts Reanalysis v5) and to a larger sample of ERA5 TCs; and Sect. 3.4 evaluates how well ERA5 captures TC intensification and gravity wave production over TC lifetimes. Sect. 5 presents a discussion of the results, and Sect. 5 provides concluding remarks.

2 Data and Methods

2.1 TC Hinnamnor and the ACCLIP campaign

On 31 August 2022 TC Hinnamnor was sampled as a target of opportunity during the ACCLIP airborne science campaign out of Osan, South Korea. The campaign's primary goal was sampling outflow from the Asian Summer Monsoon (ASM) to understand how the ASM carries anthropogenic emissions to the stratosphere (Pan et al., 2025). The campaign involved two long-range research aircraft carrying a suite of research instruments, one flying in the mid-troposphere (the NCAR Gulfstream V, 14 flights) and one in the UTLS; the NASA WB-57 (15 flights) with a median (maximum) altitude of 15.7 km (19.4 km). The WB-57 overflew Hinnamnor while the storm was classified as a Category 4 supertyphoon; it had recently intensified from Category 0 over a two day period, and briefly reached Category 5. The overflight occurred several days before a period of unusual behavior in which Hinnamnor merged with tropical depression 13W, abruptly changed direction, and then experienced rapid weakening (Wang et al., 2023; Zheng et al., 2024). The gravity wave reported here was detected as the WB-57 approached Hinnamnor on a level flight leg at 17.6–17.7 km, 2 km above cloud top (Figs. 1, S2). The aircraft then began a series of dives, precluding further opportunities to measure large-scale gravity waves.

https://doi.org/10.5194/egusphere-2026-4533
Preprint. Discussion started: 26 August 2026

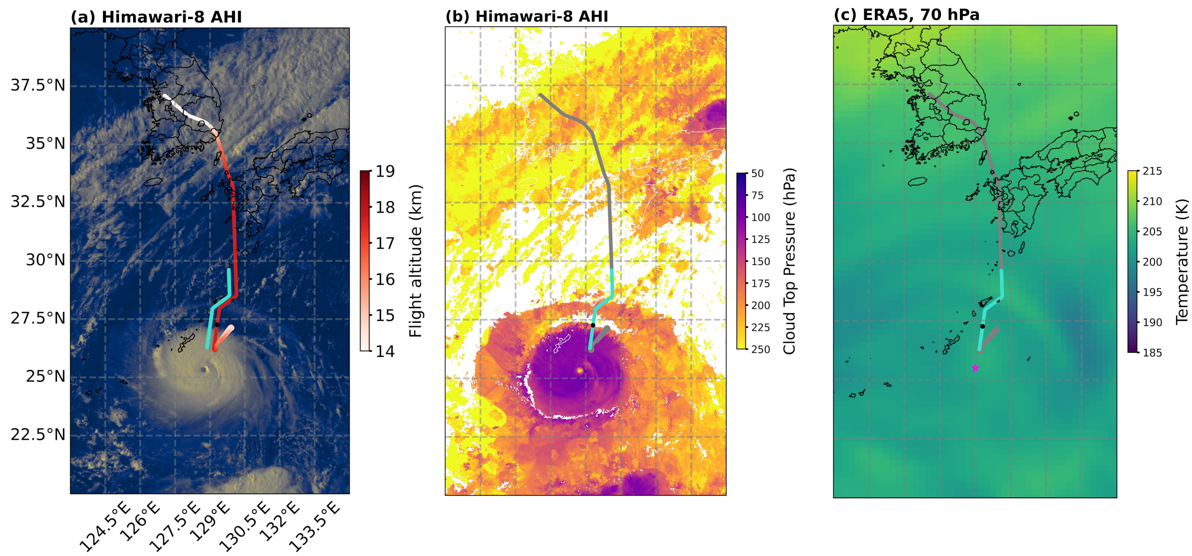

Figure 1. Temperature and cloud structures of TC Hinnamnor in satellite data and reanalysis from 31 August 2022. **a)** Flight data (outbound from Osan only), colored by altitude (km), overlaid on a Himawari-8 AHI visible (band 3) image from 07:00 UTC (Bessho et al., 2016). The turquoise portion shows the location of the hypothesized gravity wave (from 06:32:30 - 07:03 UTC), and this region is also denoted in turquoise in the following figures. In this figure, however, the turquoise portion is offset slightly from the flight path for clarity (in order to not obscure the flight altitude coloring). The black dot shows the location of the coldest temperature seen during the level leg (06:54:34 UTC). **b)** Himawari-8 AHI cloud top pressure from 07:00 UTC. Light grey shows the outbound flight path, the black dot shows the coldest in situ temperature location. The in situ temperature low is located at the edge of the cloudy region near the core. **c)** ERA5 temperature data at 70 hPa from the same geographical region at 06:00 UTC. The pink star shows the center of the TC as reported in 3 hourly IBTrACS (International Best Track Archive for Climate Stewardship) at 06:00 UTC. The ERA5 temperature field shows near-concentric rings nearly centered on the core of the TC and radiating well beyond the typhoon cloud structure.

2.2 In situ data

This study focuses on WB-57 temperature measurements, but for additional support also presents measured ozone, water vapor, and cirrus cloud presence. In situ temperature measurements on the WB-57 are provided by the Meteorological Measurement System (MMS) (Scott et al., 1990), which reports state variables such as temperature,

https://doi.org/10.5194/egusphere-2026-4533
Preprint. Discussion started: 26 August 2026

pressure, and altitude at 20 Hz frequency, yielding an effective horizontal resolution of 10 m given the ~200 ms^{-1} aircraft speed. MMS has been used on multiple high-altitude research campaigns since 1986, with reported accuracy of ±0.3 K for temperature, ±0.3 hPa for pressure, and ±15 m for altitude. We do not use MMS vertical velocities, which are more suitable for detecting small-scale structures (∼40 km or less) and strong updrafts or downdrafts (Dean-Day et al., 1998).

We use ozone measurements to help identify the presence of gravity waves, since ozone has a strong vertical gradient in the UTLS and is a nearly passive tracer on gravity wave timescales (Pfister et al., 1986; Alexander and Pfister, 1995). During ACCLIP ozone was measured on the WB-57 by the NOAA Unmanned Aircraft System (UAS) O_3 photometer (Gao et al., 2012) via dual-beam unpolarized ultraviolet absorption. Reported intrinsic precision without flow through the cell is 1.4 ppb O_3 at 200 K and 100 hPa. Overall uncertainty for the measurements taken during this campaign is quoted at 5 % (NASA, 2022) or ~15 ppb for the flight segment we focus on in this paper.

Water vapor measurements used in this study are taken from the Chicago Water Isotope Spectrometer (ChiWIS) (Clouser et al., 2025), which uses off-axis integrated cavity output spectrometry to measure both water vapor and its isotopic composition. We use 5 second measurements here; instrument H_2O precision at this integration is 3.6 ppbv in the dry conditions of the UTLS, or ~0.1 % of ambient concentration. During ACCLIP, ChiWIS water vapor mixing ratios compare well with simultaneous measurements from the Diode Laser Hygrometer (DLH) instrument (Diskin et al., 2002), including the fine-scale structure.

Cirrus at WB-57 flight level was detected by the second-generation Cloud, Aerosol, and Precipitation Spectrometer (CAPS) (Dollner et al., 2023), which consists of two instruments that detect particles in size bins of 0.5–50 $\mu\mathrm{m}$ and from 15–930 $\mu\mathrm{m}$. The CAPS retrieval provides standardized Cloud Indicator flags for the presence of liquid, mixed phase, and cirrus clouds. For clouds at other altitudes, we show data from Roscoe, the NASA Goddard Space Flight Center's Cloud Physics Lidar (McGill et al., 2002), which uses the depolarization of backscattered light at 1064 nm and 355 nm to retrieve cloud and aerosols measurements above and below the aircraft.

2.3 ERA5 reanalysis and IBTrACS

We compare TC Hinnamnor to a set of 114 broadly comparable TCs as represented in ERA5 reanalysis (Hersbach et al., 2020), a data product widely used in the atmospheric science community. The ERA5 model is run at 0.25 deg × 0.25 deg (28 km) horizontal resolution on 37 hybrid sigma-pressure model levels; in the UTLS, this corresponds to a vertical resolution of 1.8 km. Unless otherwise specified, we show output at 70 hPa (∼18.8 km over Hinnamnor),

https://doi.org/10.5194/egusphere-2026-4533
Preprint. Discussion started: 26 August 2026

which is slightly above the aircraft flight level when the gravity wave was detected (~87 hPa) and well above the level of convection. We show data from ERA5-complete (137 hybrid sigma levels) interpolated onto the flight track for the 31 August 2022 flight. We convert the model levels to pressure levels using coefficient definitions (ECMWF User Documentation, 2026) and surface pressure variable. Our sample consists of all TCs in the Western Pacific (WP) basin that reach Category 3 and above on the Saffir-Simpson scale during August–October in the twenty-two year period from 2000–2022. (An additional 181 named storms in this region and time period never reach Category 3; these are shown in the Supplement for comparison.) We define storms using the IBTrACS (International Best Track Archive for Climate Stewardship) dataset, which tracks tropical cyclones since 1940 in all ocean basins and provides wind speeds, category classification, and the latitude and longitude of storm centers every 3–6 h, depending on the monitoring agency (Knapp et al., 2010; Gahtan et al., 2024). We then use ERA5 to investigate the temperature perturbations around these TCs. (While ERA5 output is hourly, we show only those timesteps with corresponding IBTrACS data.) ERA5 storm centers can be slightly misplaced (Schenkel et al., 2017), but they have been shown to match observationally-based IBTrACS locations to $\sim$1 deg in the northern hemisphere (Hodges et al., 2017). Visual inspection also confirms that ERA5 and IBTrACS storm centers are sufficiently co-located for the purposes of this study.

For TC wind speed comparisons, we use the maximum 1 minute sustained winds reported by the U.S. Joint Typhoon Warning Center as part of IBTrACS; this temporal averaging is the basis for TC intensity definitions. Because no equivalent ERA5 output is available, we compare to the ERA5 maximum 3 second wind gusts at ten meters (computing the storm maximum value within $\sim$150 km from the IBTrACS TC center). The ERA5 gust values are estimated from model parameters and are higher than the “instantaneous” wind speeds computed at the intrinsic approximately ten minute model timestep (Morris et al., 2025). (See Fig. S3 for a comparison of ERA5 wind values for selected TCs.) All other thing being equal, they would be biased high relative to the one minute observed winds. We compute TC rapid intensification (RI) events separately for IBTrACS and ERA5 winds. To define a TC with two or more RI events, we demand that a second event be either separated by at least 48 h or that winds first decrease by at least 5 knots (kts going forward, with 1 kts = 1.94 ms^{-1}).

2.4 Methods

We use simple methodologies to estimate TC gravity wave amplitudes that are applicable both to in situ aircraft measurements along a single flight track, and to ERA5 reanalysis which shows full 2D temperature perturbation

https://doi.org/10.5194/egusphere-2026-4533
Preprint. Discussion started: 26 August 2026

patterns. While prior studies have often used spectral analysis to detect and characterize concentric TC gravity waves, with complex adjustments to handle anisotropic structures (e.g. Gong et al., 2015), these methods are not applicable to our aircraft data. We therefore rely on IBTrACS for TC locations and develop two simple metrics to characterize their gravity waves, a peak-to-peak measurement and a "trimmed metric" intended to reduce spurious outliers.

For the in situ data, our level leg approaching Hinnamnor sampled a half-wavelength, so we compute the peak-to-peak gravity wave amplitude as simply the difference between the minimum and maximum temperatures. (There is little high-frequency noise, less than 0.05 K σ.) Since the flight track is abitrary, the resulting value is conservative: it is an underestimate of the maximum gravity wave amplitude at this particular time due to anisotropy, and likely a strong underestimate of the maximum over the lifetime of the cyclone.

For ERA5 reanalysis, we apply the method discussed above along the specific flight track, and also construct metrics for each TC and timestep that allow generalized comparisons across TCs in our sample. We define an amplitude for each 3-hour time step in which the storm is classified as Category 3 or higher (2422 timesteps). We repeat this for storms that never reach Category 3 (4700 total timesteps). We first select ERA5 data in a 20 deg $\times$ 20 deg box around the IBTrACS storm center and remove any large-scale climatological temperature variations by subtracting the daily mean temperature averaged over our sample years 2000–2022. We then consider 36 transects radiating from the storm core at 10 deg intervals, each 5 degrees ($\sim$550 km) long (see Fig. S4 for a visual explanation). In Method 1 (hereafter "peak-to-peak"), we define the gravity wave activity simply as the maximum of the set of maximum - minimum amplitudes along each transect. In Method 2 (hearafter "trimmed"), we attempt to avoid outlier temperature variations that are not due to gravity wave activity. We first calculate the standard deviation of temperature along each transect, and define the gravity wave amplitude for a given timestep as the transect with a standard deviation larger than approximately 95 % of the 36 transects (34 out of 36, i.e. we reject the two transects from each storm with the largest values) and then take the maximum.

These simple metrics provide a tractable approach for comparing aircraft data with a large sample of TCs whose irregular, anisotropic, and overlapping gravity wave patterns make automated characterization difficult. Both methods are robust to slight mismatches between the IBTrACS and ERA5 storm centers. Both are appropriate for gravity wave signals that do not form a full circle or spiral around the TC core; they are agnostic to the quadrant in which maximum gravity wave activity occurs. Both are affected by the "background noise" of non-gravity-wave temperature perturbations if gravity waves are absent, but we hand-verify that our dataset is indeed dominated by concentric

https://doi.org/10.5194/egusphere-2026-4533
Preprint. Discussion started: 26 August 2026

patterns. To quantify the background, we apply the process described above to random latitude and longitude pairs, choosing one location within the Western Pacific basin for every timestep associated with a storm in our sample.

3 Results

3.1 Gravity wave activity measured during the Hinnamnor overflight

On 31 August 2022, the WB-57 measured strong temperature variations consistent with gravity wave activity while the plane flew towards TC Hinnamnor at just under 18 km (Fig. 1, 2). The aircraft was well into the overworld stratosphere, at 400 K potential temperature, and at least 2 km above the maximum cloud top altitude measured by either the on-board lidar instrument or the Himawari satellite (which reports a minimum cloud top pressure for this time period of ∼124 hPa, equivalent to 15.6 km.) During a half-hour stretch starting around 3:30 PM local time (6.514 UTC), or 367 km in horizontal distance from the TC core, aircraft measurements showed a 9.6 K drop in temperature that was strongly correlated with ozone values (Fig. 2, which shows timeseries of temperature, altitude, ozone, and water vapor for the entire flight). The background environment was sufficiently dry that the large temperature swing did not quite induce saturation – RH reaches 98 % at the coldest temperature – and water vapor remained near-constant at stratospheric values of 5.3 ppm, with no evidence of convective hydration or gravity wave dehydration.

The low temperature and high ozone extrema during this flight leg are 2.7 and 3.5 σ atypical for this altitude over the Osan campaign (from a sample of 37 means over 30 second segments at 17.6–17.8 km altitude). Comparison to the mean ozone profile suggests vertical displacements of air parcels of 0.5 km from above at the start of the leg and 0.5 km from below at the end (Fig. 3a). Purely adiabatic displacement of this magnitude would produce temperature variations of $\sim 10\ \mathrm{K\ km^{-1}}$ in an isothermal atmosphere. While the observed background temperature profile may contribute $\sim 3\ \mathrm{K\ km^{-1}}$ more (Fig. 3b), the measured amplitude is still consistent with near-adiabatic displacement.

Although the aircraft flew at a nearly constant altitude for nearly an hour and over 700 km, we identify only the second half of this period as sampling a relatively undilute gravity wave. In a plot of the ozone-temperature relationship, measurements taken between 6.514 and 7.05 UTC hours show a tightly correlated relationship distinct from the background stratosphere (Fig. 3c). The only outliers are three narrow (36 km) bands of exceptionally high ozone, up to 500 ppb, which are comparatively cool. The ozone-temperature relationship during this leg is unique

https://doi.org/10.5194/egusphere-2026-4533
Preprint. Discussion started: 26 August 2026

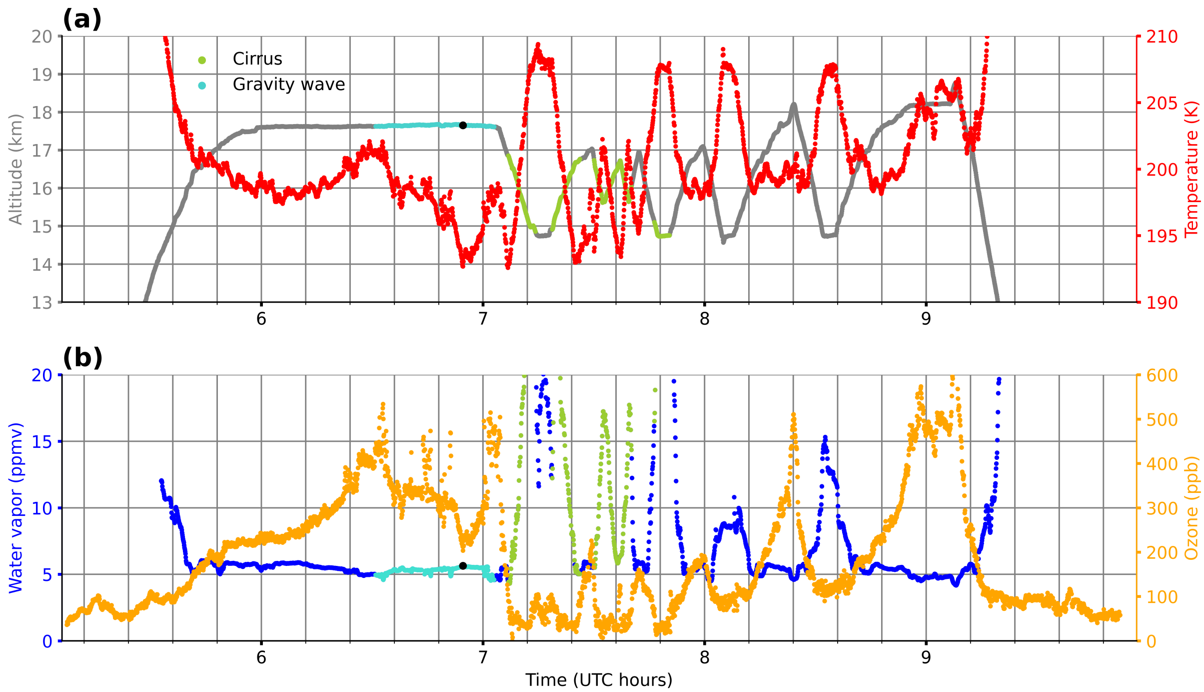

Figure 2. Time series of in situ data for the entire flight on 31 Aug. 2022, shown for context. **a)** Altitude (km) and temperature (K), with the level leg region of interest highlighted in turquoise (as in Fig. 1). Black dot marks the coldest temperature seen during this flight leg. **b)** Water vapor (ppmv) and ozone (ppb). In both panels, green denotes sampled cloud ice, seen only on dives into the Hinnamnor cloud deck. The level leg shows little variation in water vapor but strong variation in temperature and ozone explainable by the vertical displacement of a gravity wave.

across all stratospheric sampling out of Osan during ACCLIP (15 research flights). At no other time did the aircraft experience temperatures below 193 K in air with ozone above 200 ppb. This ozone-temperature relationship is a characteristic fingerprint of a stratospheric gravity wave with strong vertical displacement.

https://doi.org/10.5194/egusphere-2026-4533
Preprint. Discussion started: 26 August 2026

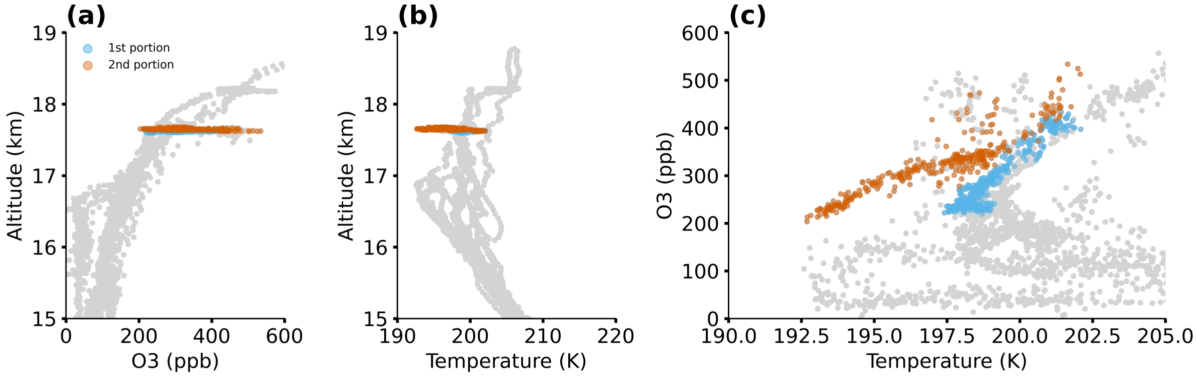

Figure 3. Temperature and ozone during the 31 Aug. 2022 flight, with the first (blue) and second (brown) portions of the level leg highlighted; brown points represent the identified gravity wave. **a)** temperature vs. altitude, **b)** ozone vs. altitude, and **c)** the ozone temperature vs. relationship, in which the gravity wave is clearly distinct from the remainder of the flight.

240 ### 3.2 Hinnamnor gravity waves in ERA5

ERA5 reanalysis shows concentric gravity waves over Hinnamnor at the time of the overflight (Fig. 1), but with substantially smaller amplitudes than that observed by the aircraft. In ERA5, the maximum perturbation interpolated along the flight track is 2.7 K, less than a third of the 9.6 K variation measured in situ (Fig. 4, which shows output from 60 and 137 vertical level versions, interpolated to the flight track; see Fig. S5 for uninterpolated data). There
245 is no suggestion that the flight track was somehow an anomalous part of the overall gravity wave pattern above Hinnamnor at this time. The measured temperature variation also exceeds peak-to-peak amplitudes in ERA5 at any time over Hinnamnor's lifetime: the maximum Hinnamnor amplitudes in ERA5, which occurs four days later, are ~9 K at 70 hPa and 8 K at 100 hPa. At least for this particular cyclone, the gravity wave amplitudes in ERA5 appear too small (See Fig. S6 for a comparison between in situ data, ERA5, and 5-km RRJ-ClimCORE reanalysis). The
250 ERA5 horizontal wavelength of ~200 km is about half the ~560 km estimated from aircraft data for the largest-scale perturbation, but both values lie within the range previously reported in the literature for TC gravity waves, which spans 40–1900 km (Table 1). The ERA5 vertical wavelength of ~3.5 km (found by considering the vertical evolution of the wave in space and time) again lies within the range previously reported for TC gravity waves.

https://doi.org/10.5194/egusphere-2026-4533
Preprint. Discussion started: 26 August 2026

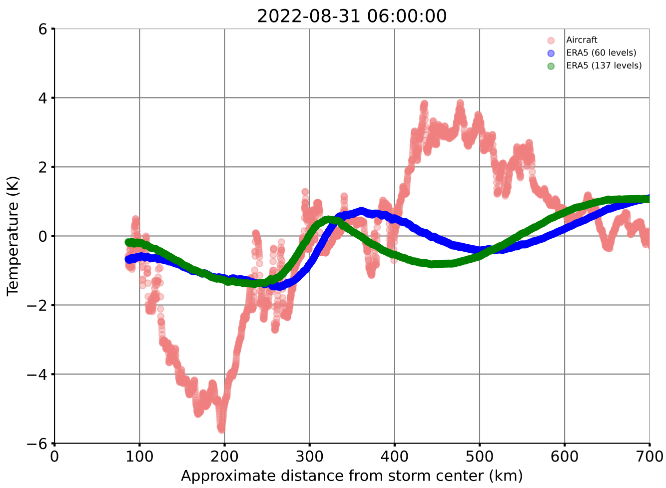

Figure 4. Temperature perturbations along the flight track near TC Hinnamnor on 31 Aug. 2022 in in situ measurements (red, 87 hPa) and in reanalysis interpolated to the flight track: ERA5 60-level (blue) and 137-level (green). Perturbations are computed as the difference from the mean over this portion of the level flight leg. The gravity wave in ERA5 shows a smaller amplitude and shorter wavelength than in in situ measurements. (Differences in phase are expected.) See Fig. S5 for non-interpolated ERA5 (showing that interpolation does not degrade the amplitude) and Fig. S6 for a 5-km renalysis product (RRJ-ClimCORE).

3.3 Comparison to the larger TC sample

Comparing the Hinnamnor overflight to our larger sample of 114 tropical cyclones in ERA5 reanalysis suggests that Hinnamnor is a typical TC in this dataset, and that the overflight occurred on a typical day in Hinnamnor's lifecycle. First, the detection of gravity waves on the overflight is not unusual. Visual inspection shows that Hinnamnor displays concentric or spiral temperature perturbations in 80 % of the timesteps when it is Category 3 and above. Gravity waves are even more prevalent in the overall sample, at 94 % probability for Category 3 and above storms (estimated using a random sample of 100 timesteps across all storms). Nearly all TCs in the sample (113 of 115, or 98 %) produce concentric or spiral temperature perturbations at some point during their lifetimes. Gravity waves are only slightly less prevalent in weaker storms, at 82 % for storms which never make it to Category 3. We are confident

https://doi.org/10.5194/egusphere-2026-4533
Preprint. Discussion started: 26 August 2026

these temperature perturbations are gravity waves since they are coincident with expected ozone and vertical velocity variations.

To evaluate Hinnamnor's gravity wave amplitudes in ERA5, we consider both methods described in Sect. 2.4, the peak-to-peak amplitude and the trimmed metric. The two are strongly correlated, with slope 0.24 (Fig. 5). Both have an identical coefficient of variation (0.29), suggesting the peak-to-peak amplitude is not overly contaminated by outliers. Using either method, Hinnamnor's gravity wave amplitudes in ERA5 are typical of the overall sample, with close to median values (Table 2 and Fig. 5, compare pink and blue dots). In addition, the overflight of 31 Aug. 2022 fell on a typical day for Hinnamnor (Fig. 5, compare green and pink dots). As mentioned above, at no time does Hinnamnor in ERA5 show gravity wave amplitudes larger than measured in situ on 31 August. See Fig. S7 for a comparison to a matched set of non-typhoon observations.

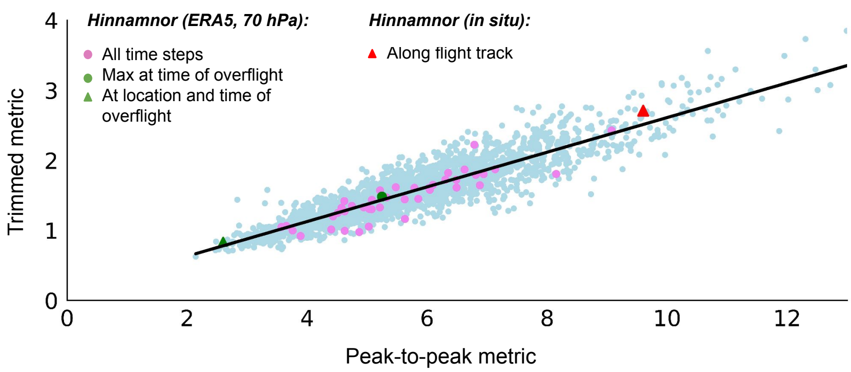

Figure 5. Comparison of TC gravity wave amplitudes across storms and across metrics (peak-to-peak amplitude and trimmed metric), using ERA5 at 70 hPa. The two metrics scale well with each other, with a slope of 0.24. Blue dots = the maximum gravity wave amplitude for each TC in our sample at each timestep. Pink dots = all instances of TC Hinnamnor in ERA5; green dot = the time of the overflight on 31 Aug. 2022. Triangles show the value on the *actual overflight transect* in ERA5 (green) and aircraft measurements (red). The median trimmed metric is 1.49 K for all TC observations at 70 mb and 1.44 K for Hinnamnor. (Analogous peak-to-peak values are 5.53 and 5.28 K, respectively.) These data imply that Hinnamnor is a typical TC regarding gravity wave activity according to our metrics, that the overflight occurred at a representative time, and that the aircraft temperature measurements are discrepant with ERA5. See Fig. S7 for a comparison to a matched set of non-typhoon observations.

https://doi.org/10.5194/egusphere-2026-4533
Preprint. Discussion started: 26 August 2026

	Hinnamnor overflight		ERA5 (max transects)	
	Aircraft	ERA5	TCs, all timesteps	random locations
Peak-to-peak	9.7	5.28	5.53	4.01
Trimmed metric	2.54	1.44	1.49	1.17
Ratio	3.81	3.67	3.71	3.42

Table 2. GW temperature amplitudes in both peak-to-peak and trimmed metrics. Left section compares the Hinnamnor overlight in in situ measurements and in ERA5 at 70 hPa. Right section compares mean 70 hPa values in our sample of ERA5 TCs when they are Category 3 or above and in our paired random background sample. (We compute the maximum transect value at each timestep, then take the median of the distribution.) Hinnamnor in ERA5 lies close to the median ERA5 TC value. The ratio of the metrics is broadly consistent across all TCs but differs from that in background "noise", as would be expected. TCs that never reach Category 3 have a smaller median gravity wave amplitude, at 1.39 in the trimmed metric.

Since our two metrics are consistent, we choose one (the trimmed metric) and show the distribution of ERA5 TC gravity wave amplitudes in our sample in Fig. 6 (using all timesteps for storms of Category 3 and above). The distribution is slightly right-skewed, with the higher values in the tail all reflecting true concentric gravity wave activity rather than artifacts. Hinnamnor's overall patterns are visually similar to other TCs (see snapshots in Fig. 6, which include four other representative TCs, and Fig. S8 for all TCs in our sample), and its ERA5 gravity wave amplitude on 31 Aug. lies in the 44th percentile. The measured in situ amplitude, by contrast, would fall in the 97th percentile. The comparison suggests that ERA5 systematically underestimates TC gravity wave amplitudes.

https://doi.org/10.5194/egusphere-2026-4533
Preprint. Discussion started: 26 August 2026

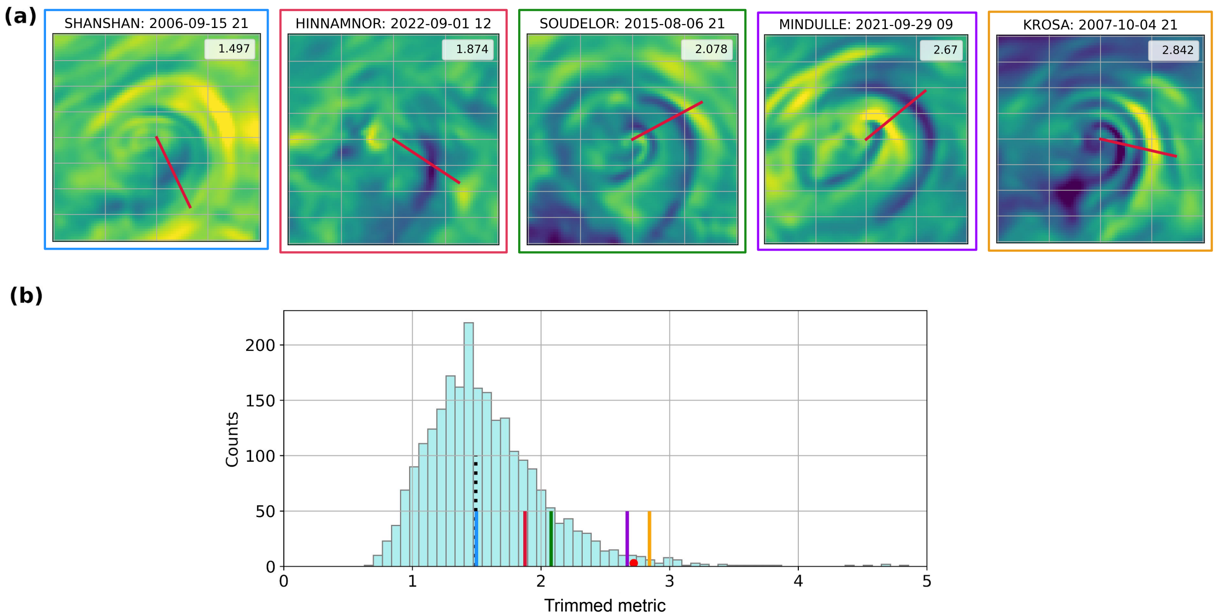

Figure 6. Histogram of TC GW trimmed metric amplitudes in our ERA5 sample (115 TCs, 2422 total time steps at Category 3 and above). Black dotted line shows the median value of 1.49. Vertical lines show values for selected example storms at their point of lifetime strongest GW activity, with snapshots above showing their temperature fields and the corresponding transect angle. (Note that the Hinnamnor image and value here are from 1 Sept. 2022, two days after the overflight; for snapshots from all storms, see Fig. S8.) Red dot shows the equivalent value from in situ measurements during the Hinnamnor overflight, which would be 97th percentile in the ERA5 distribution.

3.4 Evolution of TC intensity and GW amplitudes

While Hinnamnor is a typical TC in ERA5 reanalysis, it is important to assess whether its behavior on the day of the flight was subject to unusual real-world factors that ERA5 did not capture. TC GW amplitudes are expected to increase during periods of rapid intensification, and TC Hinnamnor did in fact strengthen significantly shortly before the in situ measurements were obtained. Observed wind speeds tripled over the 48 h of 28–29 Aug., from ~40–120

https://doi.org/10.5194/egusphere-2026-4533
Preprint. Discussion started: 26 August 2026

kts; a day later Hinnamnor briefly reached Category 5, with wind speeds nearly 140 kts. The 31 Aug. overflight would therefore be a time to expect large gravity waves.

Hinnamnor's intensification is strong but not an outlier for our sample, at 94th percentile for maximum positive wind change in 24 h (Fig. 7a). In ERA5, however, TC winds are much smaller and grow more slowly and steadily, both for Hinnamnor and across the entire sample (Fig. 7b; see Fig S9 for further evidence that Hinnamnor is not an outlier in ERA5 and IBTrACS). Note that this comparison should favor ERA5, since it compares ERA5 maximum 3 second wind gusts to observed 1 minute sustained winds (see Sect. 2.3); instead ERA5 values are lower. In IBTrACS observations, $\sim$79 % of TCs experience rapid intensification (RI) at least once, and $\sim$18 % experience two RI episodes, using the standard definition of a 30 kt increase over 24 h. In ERA5, only 14 % exhibit one RI episode, and none experience two. The near-absence of rapid intensification in ERA5 remains even if RI is re-defined based on fractional rather than absolute changes in wind speed (Table 3). This misrepresentation of TC evolution in ERA5 should therefore produce a general low bias in their gravity wave production not limited to Hinnamnor.

The evolution of TC gravity waves in ERA5 TCs does indeed differ from the intermittent production reported in observational studies. Without the complication of rapid intensification, ERA5 gravity wave amplitudes tend to gradually increase over the lifetime of a storm, as wind speeds do (Fig. 8). ERA5 gravity wave amplitude in our sample is therefore weakly correlated with wind speed (i.e. TC intensity), at $r = 0.27$. By contrast, the weaker storms in our study region, those that never reach Category 3, have weaker gravity wave amplitudes (in the trimmed metric, median of 1.39 vs. 1.49 for Category 3 and above) which decrease slightly over storm lifetime (Fig. S10), implying again that wind speed is a relevant factor. These results imply that ERA5's inability to realistically capture TC winds and intensification will lead to overly weak TC GWs.

https://doi.org/10.5194/egusphere-2026-4533
Preprint. Discussion started: 26 August 2026

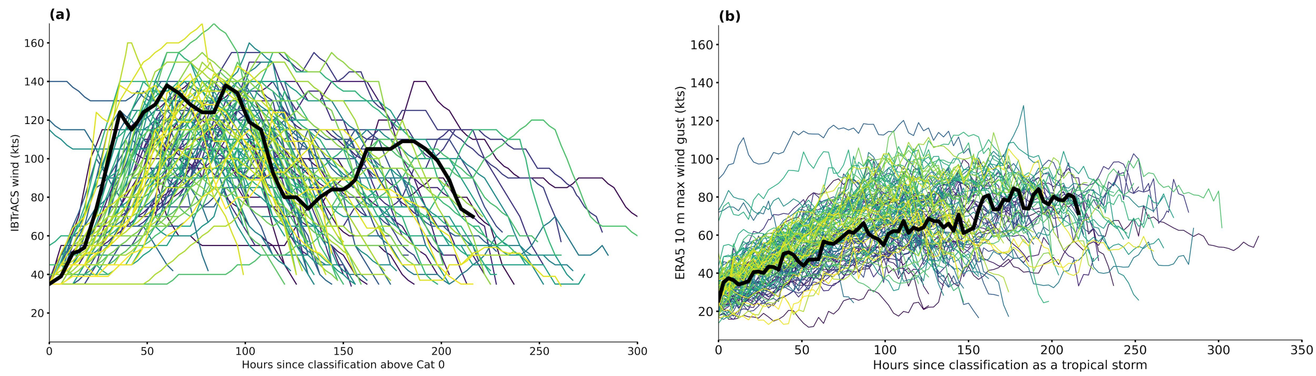

Figure 7. Evolution of wind speeds for all TCs in our sample. **a)** IBTrACS (as maximum sustained 1-minute horizontal winds), **b)** ERA5 (as maximum 3 second wind gusts in each 1-hour interval). Each line shows the evolution of one storm in the sample, with arbitrary colors other than Hinnamnor (thick black line). All times are normalized to the first hour a TC becomes a Category 0 tropical storm in IBTrACS. ERA5 3 second wind gusts are lower than 1 minute observed winds, and increase more slowly and steadily. Most TCs show rapid intensification (+30 kts in 24 h) in observations, but few do in ERA5.

Rapid intensification (out of 115 TCs)						
	Time period: 24 h			Time period: 48 h		
	+30 kts	Doubling	Max wind change	+30 kts	Doubling	Max wind change
IBTrACS	**91**	45	105 kts	112	104	117 kts
ERA5	**16**	13	45 kts	72	48	55 kts

Table 3. Frequency of rapid intensification (RI) in TCs in IBTRaCS observations and in ERA5 reanalysis in our sample of 115 storms. We show both the standard definition (+30 kts in 24 h) and alternate definitions to accommodate the apparent low bias of ERA5 winds. The maximum absolute wind speed changes in ERA5 are less than half those from IBTrACS, because ERA5 wind speeds are both biased low and too stable. Under the standard RI definition, nearly 80 % of TCs in our sample experience RI (from IBTrACS) but less than 15 % do in ERA5. This difference persists even with alternate definitions of RI based on relative wind speeds. See Li et al. (2022b) for the merits of alternative definitions.

https://doi.org/10.5194/egusphere-2026-4533
Preprint. Discussion started: 26 August 2026

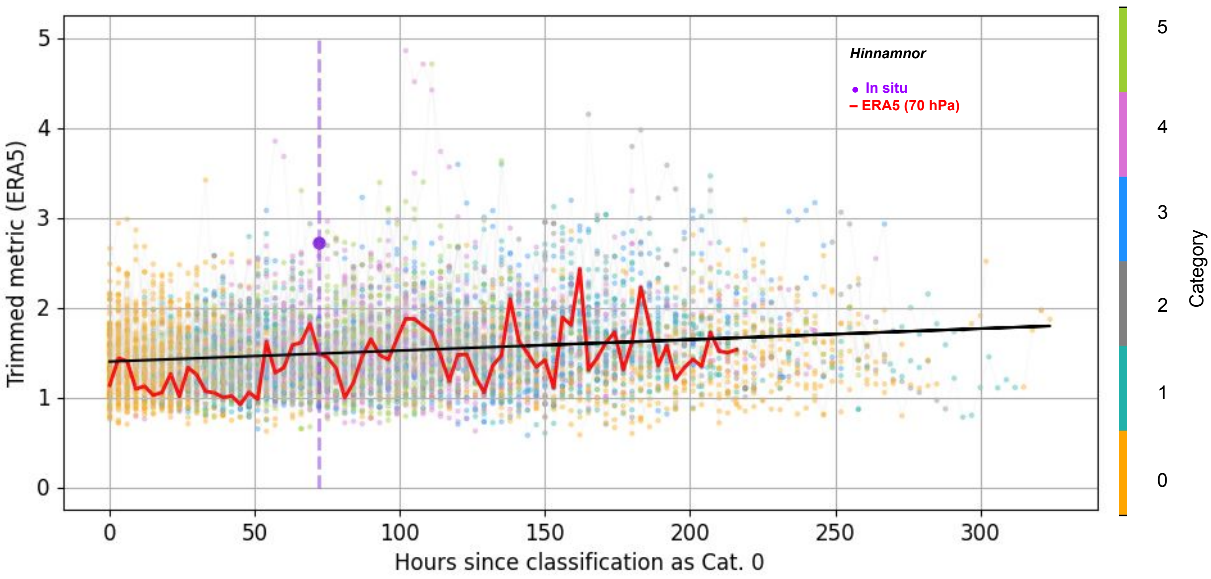

Figure 8. TC GW amplitude in our sample in ERA5 (trimmed metric) as a function of hours since classification as a tropical storm. Sample is restricted to storms that reach Category 3 but the figure includes timesteps at Category 0–2. Points are colored by TC category. Red line is TC Hinnamnor at 70 hPa in ERA5; purple dot shows the in situ measurement (2.54) at the time of overflight (dotted vertical line). ERA5 values are effectively biased high since they are taken on the optimal transect angle, but the overflight timestep (72 h since classification as a tropical storm) remains far lower than the in situ measurement. Black line shows a least-squares fit through all ERA5 points (m = 0.0012, b = 1.39). The slight increase in gravity wave activity over time is likely related to their strengthening intensities. Storms that never reach category 3 do not show this trend (Fig. S10).

https://doi.org/10.5194/egusphere-2026-4533
Preprint. Discussion started: 26 August 2026

4 Summary

This work describes new in situ measurements of a large-scale gravity-wave-induced temperature fluctuation over a tropical cyclone, obtained on one of only a few overflights described in the literature (e.g. Pfister et al., 1993). The gravity wave observed over TC Hinnamnor during ACCLIP was extremely large (9.6 K peak-to-peak); contemporaneous ERA5 reanalysis produced a much smaller amplitude (2.6 K). In general, while ERA5 TCs show near-ubiquitous production of spiral and concentric gravity waves (88 % for storms at Category 3 or above), their amplitudes appear too small. One reason for this low bias may be ERA5's inability to realistically represent aspects of TC winds that affect gravity waves. Prior studies have found that reanalyses do not accurately capture TC wind speeds (e.g. Schenkel and Hart, 2012) or intensification (Roberts et al., 2020; Baker et al., 2024), but the repercussions on gravity wave properties may not have been fully appreciated.

5 Discussion

The results presented in this paper, and those compared in Table 1, suggest that nearly all studies of TC gravity waves are limited by resolution, either horizontal or vertical. Model and reanalysis studies at horizontal resolutions greater than or equal to 30 km cannot reproduce TC intensification. Satellite-based observational studies at vertical resolutions greater than or equal to 3 km blur the short-vertical-wavelength gravity waves typically produced by TCs. The solution might seem to be ultra-high-resolution models, which have been shown to produce realistic rapid intensification events in TCs (Baker et al., 2024; Huang et al., 2024). These models do produce stronger TC gravity waves, with peak-to-peak amplitudes averaging 5.0 K vs. 3.8 K for reanalysis and 1.2 K for satellite-based studies, closer to the values from the few aircraft overflights we have.

High-resolution models do however still appear to struggle with some TC gravity wave characteristics. First, they disagree with each other on basic storm properties. In a study of nine global storm-resolving models, Judt et al. (2021) found that their TCs showed dramatic differences in intensity, compactness, eyewall size, and overall frequency. The differences are due in part to microphysics and cannot be removed by simply further increasing resolution. Resolution also continues to matter even at very fine scales. Polichtchouk et al. (2022) used a single model (ECWMWF IFS) to show that resolutions bewteen 1.25–7.8 km produced very different convective gravity wave spectra. They also showed that regardless of resolution, parametrized convection inhibits deep convective updrafts in the model and

https://doi.org/10.5194/egusphere-2026-4533
Preprint. Discussion started: 26 August 2026

therefore reduces gravity wave production. Possibly for this reason, a case study of TC-Hinnamnor using the new RRJ-ClimCORE reanalysis, which has 5-km horizontal resolution but parameterized convection (Nakamura et al., 2022), found relatively weak gravity wave activity, with amplitude along the 31 August flight track only one third the observed value (∼3 K vs. 9.6 K; see Fig. S6, similar to that seen in ERA5). More systematic study would be needed to determine whether RRJ-ClimCORE underestimates gravity wave amplitudes in general or specically during periods of exceptionally strong activity, such as those after rapid intensification events which are difficult to model.

The problems with measured and modeled TC gravity waves are difficult to overcome at present. For other difficult-to-model TC properties, researchers have successfully combined datasets to remove biases. TC sizes in reanalysis are regularly corrected using machine learning methods trained on satellite data (e.g. Bian et al., 2021), and recently TC intensities have been adjusted by a similar approach (Xu et al., 2024; Liu et al., 2025). Intensity adjustment is possible because real-world TC wind speeds are readily measured using dropsondes or radar, or in satellite imagery by feature tracking or proxies such as lightning (e.g. Zhang et al., 2015; Hoffmann et al., 2018; Knaff et al., 2018; Wright, 2019). For TC-related stratospheric gravity waves, however, there is as yet no observational ground truth, since aircraft overflights are too scarce and AIRS satellite retrievals too coarse. Establishing a larger sample of fine-scale observations of TC gravity waves should be a priority. Two potential options are the lidar-based approach of the 2025 CG WaveS aircraft campaign, or radio occultations using the global navigation satellite system (GNSS-RO), which are sensitive to smaller vertical wavelengths than AIRS, down to ∼ 2 km (Ratynski et al., 2025). GNSS-RO data from the COSMIC-2 satellites have recently been used to detect stratospheric gravity waves associated with three TCs (Wang et al., 2026); three published example profiles show amplitudes of ∼3–5 K, similar to or larger than co-located ERA5 profiles. Sampling over a larger number of TCs could provide the training data needed to construct accurate global datasets.

Accurately representing TC gravity waves in models is important for understanding future changes in stratospheric water vapor. At present, tropical cyclones are believed to generate ∼ 30 % of strongly overshooting convective events (Romps and Kuang, 2009) and drive over ∼10 % of troposphere-to-stratosphere mass transport (Zhan and Wang, 2012). While TCs dry the tropopause, they deposit significant amounts of water above it in the lower stratosphere (Ray and Rosenlof, 2007; Ravindra Babu et al., 2015; Venkat Ratnam et al., 2016; Jiang et al., 2020; Carbone et al., 2025), with the strongest TCs producing the largest perturbations (Fagan and Homeyer, 2025). These water enhancements are modulated by induced TC gravity waves, which produce cirrus as high as 18 km altitude (Pandit et al., 2024); e fforts are underway to capture these effects in models (e.g. Dolaptchiev et al., 2023). In future warmer

https://doi.org/10.5194/egusphere-2026-4533
Preprint. Discussion started: 26 August 2026

climate conditions, TCs are expected to increase in intensity (Emanuel, 2005; Elsner et al., 2008) and to experience more rapid intensification events (Song et al., 2021; Manikanta et al., 2023), amplifying both upward water transport and subsequent gravity wave dehydration. Understanding the net effect of these competing processes requires accurate representation of TC gravity waves. The results reported here suggest our current tools underestimate their amplitudes and their dehydration potential.

https://doi.org/10.5194/egusphere-2026-4533
Preprint. Discussion started: 26 August 2026

Code availability. Code and processed data files are available upon request.

Data availability. ACCLIP measurements: MMS temperatures, CAPS cloud presence, ChiWIS water vapor, Roscoe, and UAS O_3 are available on the NASA LARC site (https://www-air.larc.nasa.gov/). ERA5 data can be found at the Climate Data Store (https://cds.climate.copernicus.eu/datasets/reanalysis-era5-pressure-levels?tab=download) and the IBTrACS dataset at https://www.ncei.noaa.gov/access/metadata/landing-page/bin/iso?id=gov.noaa.ncdc:C01552. Himawari raw radiance data as netcdf files can be found on JAXA's FTP server: https://www.eorc.jaxa.jp/ptree/ and Himawari cloud top data at https://noaa-himawari8.s3.amazonaws.com/index.html#AHI-L2-FLDK-Clouds/.

Author contributions. In situ measurements were provided by TB and JD (MMS); and BC, CK, AD, and EM (ChiWIS). RRJ-ClimCORE reanalysis data and procesing provided by SW, RU, and HN. CK performed the analysis, with input from EM, BC, and JF. CK and EM prepared the manuscript, with comments from all co-authors.

Competing interests. The authors declare no competing interests.

Acknowledgements. CK and BC acknowledge support from the NSF Partnerships in International Research and Education program, grant number OISE-1743753. RU was supported by NASA Upper Atmosphere Composition Observations Program. SW and HN are supported by Japan Science and Technology Agency (JST) through COI-NEXT (JPMJPF2013). The ACCLIP campaign was supported by NSF, NASA, and NOAA and led by L. Pan (NCAR) and P. Newman (NASA). ACCLIP ozone data was provided by T. Thornberry, and ACCLIP CAPS cirrus data by M. Dollner and B. Weinzierl. We acknowledge the whole ACCLIP team for their efforts. We thank N. Nakamura for suggestions and comments on the manuscript. CK: This work is dedicated to my mom, Hillary S. Stern (1957–2024), and my grandma, Judith Stern (1930–2023).

References

Aberson, S. D., Black, M. L., Black, R. A., Burpee, R. W., Cione, J. J., Landsea, C. W., and Marks, F. D.: THIRTY YEARS OF TROPICAL CYCLONE RESEARCH WITH THE NOAA P-3 AIRCRAFT, https://doi.org/10.1175/BAMS-87-8-1039, 2006.

Alexander, M. J. and Barnet, C.: Using Satellite Observations to Constrain Parameterizations of Gravity Wave Effects for Global Models, https://doi.org/10.1175/JAS3897.1, 2007.

Alexander, M. J. and Pfister, L.: Gravity wave momentum flux in the lower stratosphere over convection, Geophysical Research Letters, 22, 2029–2032, https://doi.org/10.1029/95GL01984, 1995.

Atlas, R. and Bretherton, C. S.: Aircraft observations of gravity wave activity and turbulence in the tropical tropopause layer: prevalence, influence on cirrus clouds, and comparison with global storm-resolving models, Atmospheric Chemistry and Physics, 23, 4009–4030, https://doi.org/10.5194/acp-23-4009-2023, 2023.

Baker, A. J., Vannière, B., and Vidale, P. L.: On the Realism of Tropical Cyclone Intensification in Global Storm-Resolving Climate Models, Geophysical Research Letters, 51, e2024GL109 841, https://doi.org/10.1029/2024GL109841, _eprint: https://agupubs.onlinelibrary.wiley.com/doi/pdf/10.1029/2024GL109841, 2024.

Beres, J. H., Alexander, M. J., and Holton, J. R.: Effects of Tropospheric Wind Shear on the Spectrum of Convectively Generated Gravity Waves, https://journals.ametsoc.org/view/journals/atsc/59/11/1520-0469_2002_059_1805_eotwso_2.0.co_2.xml, 2002.

Bessho, K., Date, K., Hayashi, M., Ikeda, A., Imai, T., Inoue, H., Kumagai, Y., Miyakawa, T., Murata, H., Ohno, T., Okuyama, A., Oyama, R., Sasaki, Y., Shimazu, Y., Shimoji, K., Sumida, Y., Suzuki, M., Taniguchi, H., Tsuchiyama, H., Uesawa, D., Yokota, H., and Yoshida, R.: An Introduction to Himawari-8/9— Japan’s New-Generation Geostationary Meteorological Satellites, Journal of the Meteorological Society of Japan. Ser. II, 94, 151–183, https://doi.org/10.2151/jmsj.2016-009, 2016.

Bian, G.-F., Nie, G.-Z., and Qiu, X.: How well is outer tropical cyclone size represented in the ERA5 reanalysis dataset?, Atmospheric Research, 249, 105 339, https://doi.org/10.1016/j.atmosres.2020.105339, 2021.

Braun, S. A., Newman, P. A., and Heymsfield, G. M.: NASA's Hurricane and Severe Storm Sentinel (HS3) Investigation, https://doi.org/10.1175/BAMS-D-15-00186.1, 2016.

Cairo, F., Buontempo, C., MacKenzie, A. R., Schiller, C., Volk, C. M., Adriani, A., Mitev, V., Matthey, R., Donfrancesco, G. D., Oulanovsky, A., Ravegnani, F., Yushkov, V., Snels, M., Cagnazzo, C., and Stefanutti, L.: Morphology of the tropopause layer and lower stratosphere above a tropical cyclone: a case study on cyclone Davina (1999), Atmos. Chem. Phys., 2008.

Carbone, S., D. Riviere, E., Ghysels, M., Burgalat, J., Durry, G., Amarouche, N., Podglajen, A., and Hertzog, A.: Influence of atmospheric waves and deep convection on water vapour in the equatorial lower stratosphere seen from long-duration balloon measurements, Atmospheric Chemistry and Physics, 25, 10 603–10 623, https://doi.org/10.5194/acp-25-10603-2025, 2025.

https://doi.org/10.5194/egusphere-2026-4533
Preprint. Discussion started: 26 August 2026

Chane Ming, F., Roff, G., Robert, L., and Leveau, J.: Gravity wave characteristics over Tromelin Island during the passage of cyclone Hudah, Geophysical Research Letters, 29, 18–1–18–4, https://doi.org/10.1029/2001GL013286, _eprint: https://onlinelibrary.wiley.com/doi/pdf/10.1029/2001GL013286, 2002.

Chane Ming, F., Chen, Z., and Roux, F.: Analysis of gravity-waves produced by intense tropical cyclones, Annales Geophysicae, 28, 531–547, https://doi.org/10.5194/angeo-28-531-2010, 2010.

Chane Ming, F., Ibrahim, C., Barthe, C., Jolivet, S., Keckhut, P., Liou, Y.-A., and Kuleshov, Y.: Observation and a numerical study of gravity waves during tropical cyclone Ivan (2008), Atmospheric Chemistry and Physics, 14, 641–658, https://doi.org/10.5194/acp-14-641-2014, 2014.

Chane Ming, F., Jolivet, S., Liou, Y.-A., Jégou, F., Mekies, D., and Hong, J.-S.: Elliptical Structures of Gravity Waves Produced by Typhoon Soudelor in 2015 near Taiwan, Atmosphere, 10, 260, https://doi.org/10.3390/atmos10050260, 2019.

Chang, K.-W. and L'Ecuyer, T.: Influence of gravity wave temperature anomalies and their vertical gradients on cirrus clouds in the tropical tropopause layer – a satellite-based view, Atmospheric Chemistry and Physics, 20, 12 499–12 514, https://doi.org/10.5194/acp-20-12499-2020, 2020.

Chow, K. C., Chan, K. L., and Lau, A. K. H.: Generation of Moving Spiral Bands in Tropical Cyclones, Journal of the Atmospheric Sciences, 59, 2930–2950, https://doi.org/10.1175/1520-0469(2002)059<2930:GOMSBI>2.0.CO;2, 2002.

Clouser, B. W., Sarkozy, L. C., Singer, C. E., KleinStern, C. C., Desmoulin, A., Gaeta, D., Khaykin, S., Gabbard, S., Shertz, S., and Moyer, E. J.: The airborne chicago water isotope spectrometer: an integrated cavity output spectrometer for measurements of the HDO H_2O isotopic ratio in the Asian Summer Monsoon, Atmospheric Measurement Techniques, 18, 6465–6491, https://doi.org/10.5194/amt-18-6465-2025, 2025.

Cullens, C. Y., Thurairajah, B., England, S. L., Randall, C. E., Yue, J., and Wright, C.: Observations of Typhoon Generated Gravity Waves From the CIPS and AIRS Instruments and Comparison to the High-Resolution ECMWF Model, Journal of Geophysical Research: Atmospheres, 128, e2022JD038 170, https://doi.org/10.1029/2022JD038170, _eprint: https://onlinelibrary.wiley.com/doi/pdf/10.1029/2022JD038170, 2023.

Dean-Day, J., Chan, K. R., Bowen, S. W., Bui, T. P., Gary, B. L., and Mahoney, M. J.: Dynamics of Rocky Mountain lee waves observed during SUCCESS, Geophysical Research Letters, 25, 1351–1354, https://doi.org/10.1029/98GL01004, _eprint: https://agupubs.onlinelibrary.wiley.com/doi/pdf/10.1029/98GL01004, 1998.

Dhaka, S. K., Takahashi, M., Shibagaki, Y., Yamanaka, M. D., and Fukao, S.: Gravity wave generation in the lower stratosphere due to passage of the typhoon 9426 (Orchid) observed by the MU radar at Shigaraki (34.85°N, 136.10°E), Journal of Geophysical Research: Atmospheres, 108, https://doi.org/10.1029/2003JD003489, _eprint: https://onlinelibrary.wiley.com/doi/pdf/10.1029/2003JD003489, 2003.

Dinh, T., Podglajen, A., Hertzog, A., Legras, B., and Plougonven, R.: Effect of gravity wave temperature fluctuations on homogeneous ice nucleation in the tropical tropopause layer, Atmospheric Chemistry and Physics, 16, 35–46, https://doi.org/10.5194/acp-16-35-2016, 2016.

Diskin, G. S., Podolske, J. R., Sachse, G. W., and Slate, T. A.: Open-path airborne tunable diode laser hygrometer, in: Diode Lasers and Applications in Atmospheric Sensing, vol. 4817, pp. 196–204, https://doi.org/10.1117/12.453736, 2002.

Dolaptchiev, S. I., Spichtinger, P., Baumgartner, M., and Achatz, U.: Interactions between Gravity Waves and Cirrus Clouds: Asymptotic Modeling of Wave-Induced Ice Nucleation, https://doi.org/10.1175/JAS-D-22-0234.1, 2023.

Dollner, M., Gasteiger, J., Schöberl, M., Gattringer, A., Beres, N. D., Bui, P. T., Diskin, G., and Weinzierl, B.: The Cloud Indicator: A Novel Algorithm for Automatic Detection and Classification of Clouds Using Airborne in Situ Observations, https://doi.org/10.2139/ssrn.4654136, 2023.

ECMWF User Documentation: L137 Model Level Definitions, https://confluence.ecmwf.int/spaces/UDOC/pages/108117123/L137+model+level+definitions, accessed: 7 July 2026, 2026.

Elsner, J. B., Kossin, J. P., and Jagger, T. H.: The increasing intensity of the strongest tropical cyclones, Nature, 455, 92–95, https://doi.org/10.1038/nature07234, 2008.

Emanuel, K.: Increasing destructiveness of tropical cyclones over the past 30 years, Nature, 436, 686–688, https://doi.org/10.1038/nature03906, 2005.

Fagan, H. E. and Homeyer, C. R.: Upper Troposphere Lower Stratosphere Composition Change in Tropical Cyclones: Assessments From 17 Years of Satellite Observations, Journal of Geophysical Research: Atmospheres, 130, e2025JD044 717, https://doi.org/10.1029/2025JD044717, _eprint: https://agupubs.onlinelibrary.wiley.com/doi/pdf/10.1029/2025JD044717, 2025.

Fritts, D. C. and Alexander, M. J.: Gravity wave dynamics and effects in the middle atmosphere, Reviews of Geophysics, 41, https://doi.org/10.1029/2001RG000106, _eprint: https://onlinelibrary.wiley.com/doi/pdf/10.1029/2001RG000106, 2003.

Gahtan, J., Knapp, K., Schreck, C. I., Diamond, H., Kossin, J., and Kruck, M.: International Best Track Archive for Climate Stewardship (IBTrACS) Project, Version 4.01, https://doi.org/10.25921/82ty-9e16, 2024.

Gao, R. S., Ballard, J., Watts, L. A., Thornberry, T. D., Ciciora, S. J., McLaughlin, R. J., and Fahey, D. W.: A compact, fast UV photometer for measurement of ozone from research aircraft, Atmospheric Measurement Techniques, 5, 2201–2210, https://doi.org/10.5194/amt-5-2201-2012, 2012.

Gong, J., Yue, J., and Wu, D. L.: Global survey of concentric gravity waves in AIRS images and ECMWF analysis, Journal of Geophysical Research: Atmospheres, 120, 2210–2228, https://doi.org/10.1002/2014JD022527, _eprint: https://onlinelibrary.wiley.com/doi/pdf/10.1002/2014JD022527, 2015.

https://doi.org/10.5194/egusphere-2026-4533
Preprint. Discussion started: 26 August 2026

Hersbach, H., Bell, B., Berrisford, P., Hirahara, S., Horányi, A., Muñoz-Sabater, J., Nicolas, J., Peubey, C., Radu, R., Schepers, D., Simmons, A., Soci, C., Abdalla, S., Abellan, X., Balsamo, G., Bechtold, P., Biavati, G., Bidlot, J., Bonavita, M., De Chiara, G., Dahlgren, P., Dee, D., Diamantakis, M., Dragani, R., Flemming, J., Forbes, R., Fuentes, M., Geer, A., Haimberger, L., Healy, S., Hogan, R. J., Hólm, E., Janisková, M., Keeley, S., Laloyaux, P., Lopez, P., Lupu, C., Radnoti, G., de Rosnay, P., Rozum, I., Vamborg, F., Villaume, S., and Thépaut, J.-N.: The ERA5 global reanalysis, Quarterly Journal of the Royal Meteorological Society, 146, 1999–2049, https://doi.org/10.1002/qj.3803, _eprint: https://onlinelibrary.wiley.com/doi/pdf/10.1002/qj.3803, 2020.

Hodges, K., Cobb, A., and Vidale, P. L.: How Well Are Tropical Cyclones Represented in Reanalysis Datasets?, Journal of Climate, 30, 5243–5264, https://doi.org/10.1175/JCLI-D-16-0557.1, 2017.

Hoffmann, L. and Alexander, M. J.: Retrieval of stratospheric temperatures from Atmospheric Infrared Sounder radiance measurements for gravity wave studies, Journal of Geophysical Research: Atmospheres, 114, https://doi.org/10.1029/2008JD011241, _eprint: https://onlinelibrary.wiley.com/doi/pdf/10.1029/2008JD011241, 2009.

Hoffmann, L., Wu, X., and Alexander, M. J.: Satellite Observations of Stratospheric Gravity Waves Associated With the Intensification of Tropical Cyclones, Geophysical Research Letters, 45, 1692–1700, https://doi.org/10.1002/2017GL076123, _eprint: https://onlinelibrary.wiley.com/doi/pdf/10.1002/2017GL076123, 2018.

Huang, D., Wan, L.-f., Wan, Y.-s., Chang, S.-j., Ma, X., and Zhao, K.-j.: Gravity Wave Activity and Stratosphere-Troposphere Exchange During Typhoon Molave (2020), Journal of Tropical Meteorology, 30, 306–326, https://doi.org/10.3724/j.1006-8775.2024.026, 2024.

Jensen, E. J., Ueyama, R., Pfister, L., Bui, T. V., Alexander, M. J., Podglajen, A., Hertzog, A., Woods, S., Lawson, R. P., Kim, J.-E., and Schoeberl, M. R.: High-frequency gravity waves and homogeneous ice nucleation in tropical tropopause layer cirrus, Geophysical Research Letters, 43, 6629–6635, https://doi.org/10.1002/2016GL069426, _eprint: https://onlinelibrary.wiley.com/doi/pdf/10.1002/2016GL069426, 2016.

Jewtoukoff, V., Plougonven, R., and Hertzog, A.: Gravity waves generated by deep tropical convection: Estimates from balloon observations and mesoscale simulations, Journal of Geophysical Research: Atmospheres, 118, 9690–9707, https://doi.org/10.1002/jgrd.50781, _eprint: https://onlinelibrary.wiley.com/doi/pdf/10.1002/jgrd.50781, 2013.

Jiang, B., Lin, W., Hu, C., and Wu, Y.: Tropical cyclones impact on tropopause and the lower stratosphere vapour based on satellite data, Atmospheric Science Letters, 21, e1006, https://doi.org/10.1002/asl.1006, _eprint: https://rmets.onlinelibrary.wiley.com/doi/pdf/10.1002/asl.1006, 2020.

Judt, F., Klocke, D., Rios-Berrios, R., Vanniere, B., Ziemen, F., Auger, L., Biercamp, J., Bretherton, C., Chen, X., Düben, P., Hohenegger, C., Khairoutdinov, M., Kodama, C., Kornblueh, L., Lin, S.-J., Nakano, M., Neumann, P., Putman, W., Röber, N., Roberts, M., Satoh, M., Shibuya, R., Stevens, B., Vidale, P. L., Wedi, N., and Zhou, L.: Tropical Cyclones in Global Storm-

https://doi.org/10.5194/egusphere-2026-4533
Preprint. Discussion started: 26 August 2026

Resolving Models, Journal of the Meteorological Society of Japan. Ser. II, 99, 579–602, https://doi.org/10.2151/jmsj.2021-029, 2021.

Kim, J.-E., Alexander, M. J., Bui, T. P., Dean-Day, J. M., Lawson, R. P., Woods, S., Hlavka, D., Pfister, L., and Jensen, E. J.: Ubiquitous influence of waves on tropical high cirrus clouds, Geophysical Research Letters, 43, 5895–5901, https://doi.org/10.1002/2016GL069293, _eprint: https://onlinelibrary.wiley.com/doi/pdf/10.1002/2016GL069293, 2016.

Kim, S.-Y. and Chun, H.-Y.: Stratospheric Gravity Waves Generated by Typhoon Saomai (2006): Numerical Modeling in a Moving Frame Following the Typhoon, https://doi.org/10.1175/2010JAS3374.1, 2010.

Kim, S.-Y., Chun, H.-Y., and Wu, D. L.: A study on stratospheric gravity waves generated by Typhoon Ewiniar: Numerical simulations and satellite observations, Journal of Geophysical Research: Atmospheres, 114, https://doi.org/10.1029/2009JD011971, _eprint: https://onlinelibrary.wiley.com/doi/pdf/10.1029/2009JD011971, 2009.

Knaff, J. A., Sampson, C. R., and Musgrave, K. D.: An Operational Rapid Intensification Prediction Aid for the Western North Pacific, Weather and Forecasting, 33, 799–811, https://doi.org/10.1175/WAF-D-18-0012.1, 2018.

Knapp, K. R., Kruk, M. C., Levinson, D. H., Diamond, H. J., and Neumann, C. J.: The International Best Track Archive for Climate Stewardship (IBTrACS), https://doi.org/10.1175/2009BAMS2755.1, 2010.

Knutson, T. R., McBride, J. L., Chan, J., Emanuel, K., Holland, G., Landsea, C., Held, I., Kossin, J. P., Srivastava, A. K., and Sugi, M.: Tropical cyclones and climate change, Nature Geoscience, 3, 157–163, https://doi.org/10.1038/ngeo779, 2010.

Koteswaram, P.: ON THE STRUCTURE OF HURRICANES IN THE UPPER TROPOSPHERE AND LOWER STRATOSPHERE [1], Monthly Weather Review, 95, 541–564, https://doi.org/10.1175/1520-0493(1967)095<0541:OTSOHI>2.3.CO;2, 1967.

Kuester, M. A.: Analysis of convectively generated gravity waves within a tropical cyclone environment: Model simulation and satellite observation, Ph.D., University of Colorado at Boulder, United States – Colorado, https://www.proquest.com/docview/304889621/abstract/EB7D1BEBD4224670PQ/1, 2007.

Kuester, M. A., Alexander, M. J., and Ray, E. A.: A Model Study of Gravity Waves over Hurricane Humberto (2001), Journal of the Atmospheric Sciences, 65, 3231–3246, https://doi.org/10.1175/2008JAS2372.1, 2008.

Li, Q., Xu, J., Liu, H., Liu, X., and Yuan, W.: How do gravity waves triggered by a typhoon propagate from the troposphere to the upper atmosphere?, Atmospheric Chemistry and Physics, 22, 12 077–12 091, https://doi.org/10.5194/acp-22-12077-2022, 2022a.

Li, Y., Tang, Y., Toumi, R., and Wang, S.: Revisiting the Definition of Rapid Intensification of Tropical Cyclones by Clustering the Initial Intensity and Inner-Core Size, Journal of Geophysical Research: Atmospheres, 127, e2022JD036 870, https://doi.org/10.1029/2022JD036870, _eprint: https://agupubs.onlinelibrary.wiley.com/doi/pdf/10.1029/2022JD036870, 2022b.

Liu, G., Jiang, S., Zheng, M., Lin, S., Kong, Y., and Zhan, P.: A Global ERA5-based Tropical Cyclone Wind Field Dataset Enhanced by Integrated Parametric Correction Methods, Scientific Data, 12, 1429, https://doi.org/10.1038/s41597-025-05789-w, 2025.

Liu, H.-L., McInerney, J. M., Santos, S., Lauritzen, P. H., Taylor, M. A., and Pedatella, N. M.: Gravity waves simulated by high-resolution Whole Atmosphere Community Climate Model, Geophysical Research Letters, 41, 9106–9112, https://doi.org/10.1002/2014GL062468, _eprint: https://onlinelibrary.wiley.com/doi/pdf/10.1002/2014GL062468, 2014.

Manikanta, N. D., Joseph, S., and Naidu, C. V.: Recent global increase in multiple rapid intensification of tropical cyclones, Scientific Reports, 13, 15 949, https://doi.org/10.1038/s41598-023-43290-9, 2023.

McGill, M., Hlavka, D., Hart, W., Scott, V. S., Spinhirne, J., and Schmid, B.: Cloud Physics Lidar: instrument description and initial measurement results, Applied Optics, 41, 3725–3734, https://doi.org/10.1364/AO.41.003725, 2002.

Moon, Y., Kim, D., Camargo, S. J., Wing, A. A., Reed, K. A., Wehner, M. F., and Zhao, M.: A New Method to Construct a Horizontal Resolution-Dependent Wind Speed Adjustment Factor for Tropical Cyclones in Global Climate Model Simulations, Geophysical Research Letters, 47, e2020GL087 528, https://doi.org/10.1029/2020GL087528, _eprint: https://agupubs.onlinelibrary.wiley.com/doi/pdf/10.1029/2020GL087528, 2020.

Morris, F., Robinson, C. M., Reeder, M., Schwendike, J., Parker, D. J., Bain, C. L., and Short, C. J.: Closing the Circulation Budget, Journal of Geophysical Research: Atmospheres, 130, e2024JD041 738, https://doi.org/10.1029/2024JD041738, _eprint: https://agupubs.onlinelibrary.wiley.com/doi/pdf/10.1029/2024JD041738, 2025.

Nakamura, H., Kuma, K., Onogi, K., Miyasaka, T., Makihara, Y., Ishida, J., and Iida, M.: Toward High-Resolution Regional Atmospheric Reanalysis for Japan: An Overview of the ClimCORE Project, in: 2022 IEEE International Conference on Big Data (Big Data), pp. 6153–6158, https://doi.org/10.1109/BigData55660.2022.10020656, 2022.

NASA: ACCLIP 2022, https://www-air.larc.nasa.gov/cgi-bin/ArcView/acclip.2022#THORNBERRY.TROY/, 2022.

Pahlavan, H. A., Wallace, J. M., and Fu, Q.: Characteristics of Tropical Convective Gravity Waves Resolved by ERA5 Reanalysis, Journal of the Atmospheric Sciences, 80, 777–795, https://doi.org/10.1175/JAS-D-22-0057.1, 2023.

Pan, L. L., Atlas, E. L., Newman, P. A., Thornberry, T., Jucks, K. W., Toon, O. B., Randel, W. J., Liang, Q., Kinnison, D. E., Ueyama, R., Bresch, J. F., Honomichl, S. B., Smith, W. P., Hornbrook, R. S., Ziemba, L., Fujiwara, M., Apel, E. C., Barucci, M., Bianchini, G., Brown, M., Bui, T. P., Campos, T., Chin, M., D'Amato, F., Dean-Day, J., Diskin, G., Franchin, A., Gurganus, C., Iraci, L. T., Kim, J., Koo, J.-H., Lait, L. R., Lesko, K., Podolske, J. R., Rollins, A., Sakai, T., Shiraishi, K., Treadaway, V., Viciani, S., and Waxman, E.: The Asian Summer Monsoon Chemical and Climate Impact Project (ACCLIP): An Overview, Journal of Geophysical Research: Atmospheres, 130, e2025JD044 417, https://doi.org/10.1029/2025JD044417, _eprint: https://agupubs.onlinelibrary.wiley.com/doi/pdf/10.1029/2025JD044417, 2025.

https://doi.org/10.5194/egusphere-2026-4533
Preprint. Discussion started: 26 August 2026

Pandit, A. K., Vernier, J.-P., Fairlie, T. D., Bedka, K. M., Avery, M. A., Gadhavi, H., Venkat Ratnam, M., Dwivedi, S., Amar Jyothi, K., Wienhold, F. G., Vömel, H., Liu, H., Zhang, B., Kumar, B. S., Dinh, T., and Jayaraman, A.: Investigating the role of typhoon-induced waves and stratospheric hydration in the formation of tropopause cirrus clouds observed during the 2017 Asian monsoon, Atmospheric Chemistry and Physics, 24, 14 209–14 238, https://doi.org/10.5194/acp-24-14209-2024, 2024.

Penn, S.: Ozone and Temperature Structure in a Hurricane, Journal of Applied Meteorology, 4, 1964.

Pfister, L., Starr, W., Craig, R., Loewenstein, M., and Legg, M.: Small-Scale Motions Observed by Aircraft in the Tropical Lower Stratosphere: Evidence for Mixing and its Relationship to Large-Scale Flows, https://journals.ametsoc.org/view/journals/atsc/43/24/1520-0469_1986_043_3210_ssmoba_2_0_co_2.xml, 1986.

Pfister, L., Chan, K. R., Bui, T. P., Bowen, S., Legg, M., Gary, B., Kelly, K., Proffitt, M., and Starr, W.: Gravity waves generated by a tropical cyclone during the STEP tropical field program: A case study, Journal of Geophysical Research: Atmospheres, 98, 8611–8638, https://doi.org/10.1029/92JD01679, 1993.

Podglajen, A., Hertzog, A., Plougonven, R., and Legras, B.: Lagrangian temperature and vertical velocity fluctuations due to gravity waves in the lower stratosphere, Geophysical Research Letters, 43, 3543–3553, https://doi.org/10.1002/2016GL068148, _eprint: https://onlinelibrary.wiley.com/doi/pdf/10.1002/2016GL068148, 2016.

Polichtchouk, I., Wedi, N., and Kim, Y.-H.: Resolved gravity waves in the tropical stratosphere: Impact of horizontal resolution and deep convection parametrization, Quarterly Journal of the Royal Meteorological Society, 148, 233–251, https://doi.org/10.1002/qj.4202, _eprint: https://rmets.onlinelibrary.wiley.com/doi/pdf/10.1002/qj.4202, 2022.

Preusse, P., Ern, M., Bechtold, P., Eckermann, S. D., Kalisch, S., Trinh, Q. T., and Riese, M.: Characteristics of gravity waves resolved by ECMWF, Atmospheric Chemistry and Physics, 14, 10 483–10 508, https://doi.org/10.5194/acp-14-10483-2014, 2014.

Ratynski, M., Khaykin, S., Hauchecorne, A., Alexander, J., Mariaccia, A., Keckhut, P., and Mangin, A.: Convection-generated gravity waves in the tropical lower stratosphere from Aeolus wind profiling, GNSS-RO and ERA5 reanalysis, https://doi.org/10.5194/egusphere-2025-394, 2025.

Ravindra Babu, S., Venkat Ratnam, M., Basha, G., Krishnamurthy, B. V., and Venkateswararao, B.: Effect of tropical cyclones on the tropical tropopause parameters observed using COSMIC GPS RO data, Atmospheric Chemistry and Physics, 15, 10 239–10 249, https://doi.org/10.5194/acp-15-10239-2015, 2015.

Ray, E. A. and Rosenlof, K. H.: Hydration of the upper troposphere by tropical cyclones, Journal of Geophysical Research: Atmospheres, 112, https://doi.org/10.1029/2006JD008009, _eprint: https://onlinelibrary.wiley.com/doi/pdf/10.1029/2006JD008009, 2007.

Roberts, M. J., Camp, J., Seddon, J., Vidale, P. L., Hodges, K., Vanniere, B., Mecking, J., Haarsma, R., Bellucci, A., Scoccimarro, E., Caron, L.-P., Chauvin, F., Terray, L., Valcke, S., Moine, M.-P., Putrasahan, D., Roberts, C., Senan, R., Zarzycki, C., and

https://doi.org/10.5194/egusphere-2026-4533
Preprint. Discussion started: 26 August 2026

Ullrich, P.: Impact of Model Resolution on Tropical Cyclone Simulation Using the HighResMIP–PRIMAVERA Multimodel Ensemble, https://doi.org/10.1175/JCLI-D-19-0639.1, 2020.

Romps, D. M. and Kuang, Z.: Overshooting convection in tropical cyclones, Geophysical Research Letters, 36, https://doi.org/10.1029/2009GL037396, _eprint: https://agupubs.onlinelibrary.wiley.com/doi/pdf/10.1029/2009GL037396, 2009.

Sato, K.: Small-Scale Wind Disturbances Observed by the MU Radar during the Passage of Typhoon Kelly, Journal of the Atmospheric Sciences, 50, 518–537, https://doi.org/10.1175/1520-0469(1993)050<0518:SSWDOB>2.0.CO;2, 1993.

Schenkel, B. A. and Hart, R. E.: An Examination of Tropical Cyclone Position, Intensity, and Intensity Life Cycle within Atmospheric Reanalysis Datasets, https://doi.org/10.1175/2011JCLI4208.1, 2012.

Schenkel, B. A., Lin, N., Chavas, D., Oppenheimer, M., and Brammer, A.: Evaluating Outer Tropical Cyclone Size in Reanalysis Datasets Using QuikSCAT Data, https://doi.org/10.1175/JCLI-D-17-0122.1, 2017.

Schroeder, S., Preusse, P., Ern, M., and Riese, M.: Gravity waves resolved in ECMWF and measured by SABER, Geophysical Research Letters, 36, https://doi.org/10.1029/2008GL037054, _eprint: https://agupubs.onlinelibrary.wiley.com/doi/pdf/10.1029/2008GL037054, 2009.

Scott, S. G., Bui, T. P., Chan, K. R., and Bowen, S. W.: The Meteorological Measurement System on the NASA ER-2 Aircraft, https://journals.ametsoc.org/view/journals/atot/7/4/1520-0426_1990_007_0525_tmmsot_2_0_co_2.xml, 1990.

Shi, G., Hu, X., Yao, Z., Guo, W., Sun, M., and Gong, X.: Case study on stratospheric and mesospheric concentric gravity waves generated by deep convection, Earth and Planetary Physics, 5, eepp2021 002, https://doi.org/10.26464/epp2021002, _eprint: https://onlinelibrary.wiley.com/doi/pdf/10.26464/epp2021002, 2021.

Song, J., Klotzbach, P. J., and Duan, Y.: Increasing lifetime maximum intensity of rapidly intensifying tropical cyclones over the western North Pacific, Environmental Research Letters, 16, 034 002, https://doi.org/10.1088/1748-9326/abdbf1, 2021.

Tratt, D. M., Hackwell, J. A., Valant-Spaight, B. L., Walterscheid, R. L., Gelinas, L. J., Hecht, J. H., Swenson, C. M., Lampen, C. P., Alexander, M. J., Hoffmann, L., Nolan, D. S., Miller, S. D., Hall, J. L., Atlas, R., Marks, F. D., and Partain, P. T.: GHOST: A Satellite Mission Concept for Persistent Monitoring of Stratospheric Gravity Waves Induced by Severe Storms, Bulletin of the American Meteorological Society, https://repository.library.noaa.gov/view/noaa/19517, 2018.

Venkat Ratnam, M., Ravindra Babu, S., Das, S. S., Basha, G., Krishnamurthy, B. V., and Venkateswararao, B.: Effect of tropical cyclones on the stratosphere–troposphere exchange observed using satellite observations over the north Indian Ocean, Atmospheric Chemistry and Physics, 16, 8581–8591, https://doi.org/10.5194/acp-16-8581-2016, 2016.

Wang, Q., Zhao, D., Duan, Y., Guan, S., Dong, L., Xu, H., and Wang, H.: Super Typhoon Hinnamnor (2022) with a Record-Breaking Lifespan over the Western North Pacific, Advances in Atmospheric Sciences, pp. s00 376–023–2336–y, https://doi.org/10.1007/s00376-023-2336-y, 2023.

https://doi.org/10.5194/egusphere-2026-4533
Preprint. Discussion started: 26 August 2026

Wang, X., Zhang, L., Wang, Y., and Zhang, Y.: Influences of the Mid-Latitude Westerly Trough on Stratospheric Gravity Waves Generated by Typhoon Lekima (2019), Journal of Geophysical Research: Atmospheres, 126, e2021JD035 399, https://doi.org/10.1029/2021JD035399, _eprint: https://onlinelibrary.wiley.com/doi/pdf/10.1029/2021JD035399, 2021.

Wang, X., Wang, Y., Zhang, L., Zhang, Y., and Guan, J.: A climatology of stratospheric gravity waves induced by tropical cyclones on the northwest Pacific Ocean, npj Climate and Atmospheric Science, 7, 1–11, https://doi.org/10.1038/s41612-024-00705-2, 2024.

Wang, Y., Pagiatakis, S., and Vergados, P.: Characterizing Small-Scale Gravity Waves Generated by Hurricanes Through Convective Generation and Wind Filtering Effects, Earth and Space Science, 13, e2025EA004 790, https://doi.org/10.1029/2025EA004790, _eprint: https://agupubs.onlinelibrary.wiley.com/doi/pdf/10.1029/2025EA004790, 2026.

Wright, C. J.: Quantifying the global impact of tropical cyclone-associated gravity waves using HIRDLS, MLS, SABER and IBTrACS data, Quarterly Journal of the Royal Meteorological Society, 145, 3023–3039, https://doi.org/10.1002/qj.3602, _eprint: https://onlinelibrary.wiley.com/doi/pdf/10.1002/qj.3602, 2019.

Wu, J. F., Xue, X. H., Hoffmann, L., Dou, X. K., Li, H. M., and Chen, T. D.: A case study of typhoon-induced gravity waves and the orographic impacts related to Typhoon Mindulle (2004) over Taiwan, Journal of Geophysical Research: Atmospheres, 120, 9193–9207, https://doi.org/10.1002/2015JD023517, _eprint: https://onlinelibrary.wiley.com/doi/pdf/10.1002/2015JD023517, 2015.

Wu, X., Hoffmann, L., Wright, C. J., Hindley, N. P., Kalisch, S., Alexander, M. J., and Wang, Y.: Stratospheric Gravity Waves as a Proxy for Hurricane Intensification: A Case Study of Weather Research and Forecast Simulation for Hurricane Joaquin, Geophysical Research Letters, 49, e2021GL097 010, https://doi.org/10.1029/2021GL097010, _eprint: https://onlinelibrary.wiley.com/doi/pdf/10.1029/2021GL097010, 2022.

Xu, Z., Guo, J., Zhang, G., Ye, Y., Zhao, H., and Chen, H.: Global tropical cyclone size and intensity reconstruction dataset for 1959–2022 based on IBTrACS and ERA5 data, Earth System Science Data, 16, 5753–5766, https://doi.org/10.5194/essd-16-5753-2024, 2024.

Yue, J., Miller, S. D., Hoffmann, L., and Straka, W. C.: Stratospheric and mesospheric concentric gravity waves over tropical cyclone Mahasen: Joint AIRS and VIIRS satellite observations, Journal of Atmospheric and Solar-Terrestrial Physics, 119, 83–90, https://doi.org/10.1016/j.jastp.2014.07.003, 2014.

Zhan, R. and Wang, Y.: Contribution of tropical cyclones to stratosphere-troposphere exchange over the northwest Pacific: Estimation based on AIRS satellite retrievals and ERA-Interim data, Journal of Geophysical Research: Atmospheres, 117, https://doi.org/10.1029/2012JD017494, _eprint: https://agupubs.onlinelibrary.wiley.com/doi/pdf/10.1029/2012JD017494, 2012.

https://doi.org/10.5194/egusphere-2026-4533
Preprint. Discussion started: 26 August 2026

Zhang, W., Zhang, Y., Zheng, D., Wang, F., and Xu, L.: Relationship between lightning activity and tropical cyclone intensity over the northwest Pacific, Journal of Geophysical Research: Atmospheres, 120, 4072–4089, https://doi.org/10.1002/2014JD022334, _eprint: https://agupubs.onlinelibrary.wiley.com/doi/pdf/10.1002/2014JD022334, 2015.

Zheng, M., Zhang, Z., and Zhang, W.: How Did the Merger With a Tropical Depression Amplify the Rapid Weakening of Super Typhoon Hinnamnor (2022)?, Geophysical Research Letters, 51, e2024GL109 049, https://doi.org/10.1029/2024GL109049, _eprint: https://onlinelibrary.wiley.com/doi/pdf/10.1029/2024GL109049, 2024.